Progress In Electromagnetics Research, PIER 30, 131–156, 2001

ELECTROMAGNETIC FIELDS OF A THIN CIRCULA LOOP ANTENNA ABOVE A (UN)GROUNDED MULTI-LAYERED CHIRAL SLABS: THE NON-UNIFORM CURRENT EXCITATION

W.-Y. Yin, L.-W. Li, T.-S. Yeo, and M.-S. Leong

Department of Electrical and Computer Engineering
National University of Singapore
Singapore 119260

Abstract–The technique of dyadic Green's function (DGF) expressed in terms of the normalised cylindrical vector wave functions is adopted in this study for examining the electromagnetic fields excited by one thin circular loop antenna above a (un)grounded multi-layered chiral slabs. The current carried on such a circular loop antenna is expressed in a generalized Fourier series so as to incorporate practical situations. Thereby, exact representations of the radiated fields in both near and far zones are obtained in closed form, in a superposition of the right- and left-handed circularly polarized waves. Furthermore, numerical results are presented to show the radiation characteristics of the loop antenna in different layered chiral slab structures. The contributions of the lower- as well as higher-order current excitations to the far-zone field are examined in detail.

1. INTRODUCTION

It is known that chiral materials are characterized by three independent constitutive scalars and they exhibit intrinsic handedness in their interaction with electromagnetic waves. So far significant research progress has been achieved on various electromagnetic characteristics of artificially composite chiral materials, and much theoretical effort has been spent on the dyadic Green's function theory in chiral media [1–14]. Furthermore, the radiation characteristics of canonical sources in various chiral regions have also been investigated. For instance, (1) dipole antenna radiation in the presence of a homogeneous or a radially inhomogeneous chiral sphere was considered, (2) the radiation and scattering from a thin wire antenna in a unbounded chiral medium were analysed, and (3) electromagnetic fields excited by a circular loop antenna in a unbounded chiral medium and above a chiral half space were formulated [15–27]. Also, chirolens antennas and chiral slab polarization transformer for aperture antennas have been proposed by some researchers recently [28, 29]. In the previous studies, the dyadic Green's function (DGF) in chiral media has often been employed, and therefore, the formulations of DGF in one-, and two-layered, or radially arbitrary multi-layered cylindrical and spherical chiral regions have been successfully achieved by the eigenfunction expansion method combined with the scattering superposition principle [10–13, 22, 23].

In contrast to the previous study, the present work aims at examining the radiation characteristics of a circular loop antenna excited by harmonic currents of different orders. We know that there exist a number of publications for dealing with the electromagnetic radiation of a circular loop located in free-space or immersed in layered media, however, no one has investigated on the electromagnetic radiation due to the present model. In fact, the study of the interaction of electromagnetic waves with multi-layered chiral structures also has potential applications in the field of antenna engineering. In the following sections, the mathematical treatment is based on the DGF in the form of an eigenfunction expansion using the normalized cylindrical vector wave function. For the generalized Fourier series form of the loop current, all the field components are derived in an analytical form at first, and both far and near zones can be included. Finally, numerical examples are presented to show the non-uniform current excitation effects of a loop antenna on the variation of the far-zone field, and the chiral effect is naturally taken into account.

2. GEOMETRY OF THE PROBLEM

Fig. 1 shows the geometry of a thin circular loop antenna above a grounded multi-layered chiral slabs, and the grounded plane at $z = 0$ can be a perfectly conducting plane or without PEC plane.

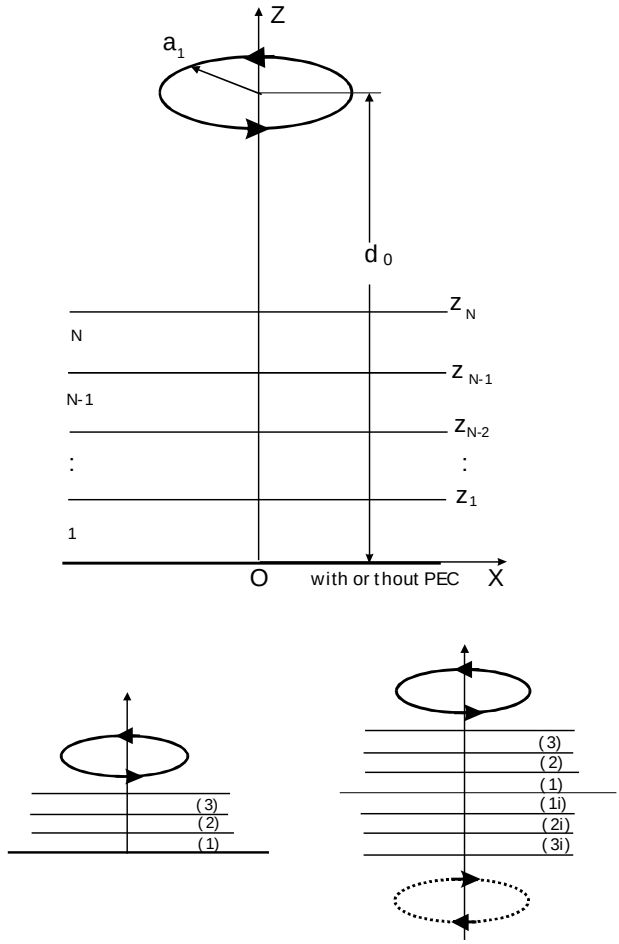

Figure 1. Geometry of a thin circular loop antenna above a (un)grounded N-layer chiral slabs.

Generally, the constitutive characteristics for each layer of the chiral slabs in frequency domain and with the time dependence $e^{-j\omega t}$ can be described by

$$\overline{D}^{(p)} = \varepsilon^{(p)} \overline{E}^{(p)} + \xi^{(p)} \overline{H}^{(p)}, \tag{1a}$$

$$\overline{B}^{(p)} = \mu^{(p)}\overline{H}^{(p)} + \eta^{(p)}\overline{E}^{(p)}, \quad p = 1, 2, \cdots, N \tag{1b}$$

where $\varepsilon^{(p)}$, and $\mu^{(p)}$ are the permittivity and permeability, respectively, and $\xi^{(p)} = \eta^{(p)^*} = j\kappa^{(p)}$ with the superscript $*$ standing for the complex conjugation and $\kappa^{(i)}$ being the chirality parameter. Here the volumetric electric current density of the thin circular loop antenna is stated as:

$$\overline{J}_1\left(\overline{R}'\right) = \frac{I(\varphi')\delta(r' - a_1)\delta(z' - d_0)}{a_1}\overline{e}'_{\varphi} \tag{2}$$

where $\overline{e}'_{\varphi}$ is the unit vector of the φ'-component with respect to the source coordinates $(r',\ \varphi',\ z')$; $I(\varphi')$ is an arbitrary function of φ' and can practically be expressed by a Fourier cosine series; a_1 is the radius of the circular loop, and the location of the circular loop is $d_0 > z_N$. Usually, the upper region $z > z_N$ is the free space $(\varepsilon_0,\ \mu_0)$.

3. GENERAL FORMULATION OF THE ELECTROMAGNETIC FIELDS

Straightforwardly, the electromagnetic fields in each layer of the grounded multi-layered chiral slabs and their upper space excited by the thin circular loop antenna are determined as follows:

$$\overline{E}^{(p)}(\overline{R}) = j\omega\mu_0 \iiint\limits_v \overline{\overline{G}}_e^{(p)}\left(\overline{R}\,|\,\overline{R}'\right) \cdot \overline{J}_1\left(\overline{R}'\right) dV', \quad p = 1, 2, \cdots, N, 0 \tag{3a}$$

$$\overline{H}^{(p)}(\overline{R}) = \iiint\limits_v \overline{\overline{G}}_{em}^{(p)}\left(\overline{R}\,|\,\overline{R}'\right) \cdot \overline{J}_1\left(\overline{R}'\right) dV' \tag{3b}$$

and

$$\overline{\overline{G}}_{em}^{(p)}\left(\overline{R}\,|\,\overline{R}'\right) = \frac{\mu_0}{\mu^{(p)}} \nabla \times \overline{\overline{G}}_e^{(p)}\left(\overline{R}\,|\,\overline{R}'\right) - \frac{j\omega\mu_0\eta^{(p)}}{\mu^{(p)}}\overline{\overline{G}}_e^{(p)}\left(\overline{R}\,|\,\overline{R}'\right) \tag{3c}$$

where the subscript v denotes the total volume occupied by the circular loop, and $\overline{\overline{G}}_e^{(p)}\left(\overline{R}\,|\,\overline{R}'\right)$ is the electric DGF corresponding to each layer of the chiral substrate. For $z > z_N$, the DGF is noted by $\overline{\overline{G}}_e^{(0)}\left(\overline{R}\,|\,\overline{R}'\right)$, where $\varepsilon^{(0)} = \varepsilon_0,\ \mu^{(0)} = \mu_0,\ \xi^{(0)} = \eta^{(0)} = 0\ (p = 0)$. By

making use of the method of scattering principle, $\overline{\overline{G}}_e^{(0)}\left(\overline{R}\,|\,\overline{R}'\right)$ consists of two parts, i.e., the unbounded DGF and the scattering DGF, as follows

$$\overline{\overline{G}}_e^{(0)}\left(\overline{R}\,|\,\overline{R}'\right)=\overline{\overline{G}}_{e0}^{(0)}\left(\overline{R}\,|\,\overline{R}'\right)+\overline{\overline{G}}_{es}^{(0)}\left(\overline{R}\,|\,\overline{R}'\right) \tag{4a}$$

where $\overline{\overline{G}}_{e0}^{(0)}\left(\overline{R}\,|\,\overline{R}'\right)$ represents the contribution of the direct waves from the loop antenna in the free space $(\varepsilon_0,\ \mu_0)$. It can be stated as:

$$\begin{aligned}&\overline{\overline{G}}_{e0}^{(0)}\left(\overline{R}\,|\,\overline{R}'\right)\\ &=-\frac{\bar{e}_z\bar{e}_z\delta\left(\overline{R}-\overline{R}'\right)}{{k_0}^2}+\frac{j}{4\pi k_0}\int_0^{+\infty}d\lambda\sum_{n=0}^{\infty}\frac{2-\delta_{n0}}{\lambda}\\ &\cdot\begin{cases}g_0\left[\overline{V}_{\substack{e\\o}n\lambda}(h_0)\overline{V}'_{\substack{e\\o}n\lambda}(-h_0)+\overline{W}_{\substack{e\\o}n\lambda}(h_0)\overline{W}'_{\substack{e\\o}n\lambda}(-h_0)\right], & z\geq z'\\ g_0\left[\overline{V}_{\substack{e\\o}n\lambda}(-h_0)\overline{V}'_{\substack{e\\o}n\lambda}(h_0)+\overline{W}_{\substack{e\\o}n\lambda}(-h_0)\overline{W}'_{\substack{e\\o}n\lambda}(h_0)\right], & z\leq z'\end{cases}\end{aligned} \tag{4b}$$

where $\bar{e}_z$ is the unit vector of the z-coordinate in the coordinate system $(r,\ \varphi,\ z)$, $\delta\left(\overline{R}-\overline{R}'\right)$ is the Dirac delta function, and $k_0^2=\omega^2\mu_0\varepsilon_0$, $g_0=\dfrac{k_0}{h_0}$, $h_0^2=k_0^2-\lambda^2$. The $\overline{\overline{G}}_{es}^{(0)}\left(\overline{R}\,|\,\overline{R}'\right)$ in (4a) describes an additional contribution of the multiple reflection wave from the boundary $z=z_N$, and can be further expressed as

$$\begin{aligned}\overline{\overline{G}}_{es}^{(0)}\left(\overline{R}\,|\,\overline{R}'\right)=\sum_{n=0}^{+\infty}\int_0^{+\infty}g^{(0)}C^{(0)}d\lambda\Big\{&\Big[A_1^{(0)}\overline{V}_{\substack{e\\o}n\lambda}(h_0)\\ &+A_2^{(0)}\overline{W}_{\substack{e\\o}n\lambda}(h_0)\Big]\overline{V}'_{\substack{e\\o}n\lambda}(h_0)+\Big[A_3^{(0)}\overline{V}_{\substack{e\\o}n\lambda}(h_0)\\ &+A_4^{(0)}\overline{W}_{\substack{e\\o}n\lambda}(h_0)\Big]\overline{W}'_{\substack{e\\o}n\lambda}(h_0)\Big\}\qquad z\geq z_N.\end{aligned} \tag{5}$$

In the pth layer $(z_{p-1}<z\leq z_p,\ p=1,2,\cdots,N;\ z_0=0)$, we have

$$\begin{aligned}&\overline{\overline{G}}_e^{(p)}\left(\overline{R}\,|\,\overline{R}'\right)\\ &=\sum_{n=0}^{+\infty}\int_0^{+\infty}g^{(0)}C^{(0)}d\lambda\left\{\left[A_1^{(p)}\overline{V}_{\substack{e\\o}n\lambda}\left(-h_+^{(p)}\right)+A_2^{(p)}\overline{W}_{\substack{e\\o}n\lambda}\left(-h_-^{(p)}\right)\right]\overline{V}'_{\substack{e\\o}n\lambda}(h_0)\right.\end{aligned}$$

$$+\left[A_3^{(p)}\overline{V}_{\substack{e\\o}n\lambda}\left(-h_+^{(p)}\right)+A_4^{(p)}\overline{W}_{\substack{e\\o}n\lambda}\left(-h_-^{(p)}\right)\right]\overline{W}'_{\substack{e\\o}n\lambda}(h_0)$$
$$+\left[A_5^{(p)}\overline{V}_{\substack{e\\o}n\lambda}\left(h_+^{(p)}\right)+A_6^{(p)}\overline{W}_{\substack{e\\o}n\lambda}\left(h_-^{(p)}\right)\right]\overline{V}'_{\substack{e\\o}n\lambda}(h_0)$$
$$+\left[A_7^{(p)}\overline{V}_{\substack{e\\o}n\lambda}\left(h_+^{(p)}\right)+A_8^{(p)}\overline{W}_{\substack{e\\o}n\lambda}\left(h_-^{(p)}\right)\right]\overline{W}'_{\substack{e\\o}n\lambda}(h_0)\Big\} \tag{6}$$

where

$$C^{(0)}=\frac{j(2-\delta_{n0})}{4\pi k_0\lambda}, \tag{7a}$$

$$k_\pm^{(p)}=\pm\frac{j\omega\left[\eta^{(p)}-\xi^{(p)}\right]}{2}+\omega\sqrt{\varepsilon^{(p)}\mu^{(p)}-\frac{\left[\xi^{(p)}+\eta^{(p)}\right]^2}{4}}; \tag{7b, c}$$

while $h_\pm^{(p)^2}=k_\pm^{(p)^2}-\lambda^2(p=1,\cdots,N)$, and $\delta_{n0}=\begin{cases}1 & n=0\\ 0 & n\neq 0\end{cases}$. $k_\pm^{(p)}$ are the wavenumbers corresponding to two circularly polarised modes supported in the pth chiral layer, i.e., the right- and left-handed circularly polarised waves (RCP: +; LCP: −) . It should be pointed out that (7b, c) can be further simplified by taking $\xi^{(p)}=\eta^{(p)^*}=j\kappa^{(p)}$ into account. Without loss of any generality, we would like to keep such a generalised form, and that

1. the definitions and orthogonal properties of the normalised cylindrical vector wave functions $\overline{V}_{\substack{e\\o}n\lambda}\left(\pm h_+^{(p)}\right)$, $\overline{V}'_{\substack{e\\o}n\lambda}\left(\pm h_+^{(p)}\right)$, $\overline{W}_{\substack{e\\o}n\lambda}\left(\pm h_-^{(p)}\right)$ and $\overline{W}'_{\substack{e\\o}n\lambda}\left(\pm h_-^{(p)}\right)$ can be found in [22], and the prime in (4)–(6) indicates the coordinates of the source;
2. using $\left\{\overline{V}_{\substack{e\\o}n\lambda}\left(\pm h_+^{(p)}\right),\ \overline{V}'_{\substack{e\\o}n\lambda}\left(\pm h_+^{(p)}\right),\ \overline{W}_{\substack{e\\o}n\lambda}\left(\pm h_-^{(p)}\right),\ \overline{W}'_{\substack{e\\o}n\lambda}\left(\pm h_-^{(p)}\right)\right\}$ instead of $\left\{\overline{M}_{\substack{e\\o}n\lambda}\left(\pm h_+^{(p)}\right),\ \overline{M}'_{\substack{e\\o}n\lambda}\left(\pm h_+^{(p)}\right),\ \overline{N}_{\substack{e\\o}n\lambda}\left(\pm h_-^{(p)}\right),\ \overline{N}'_{\substack{e\\o}n\lambda}\left(\pm h_-^{(p)}\right)\right\}$ the constructed DGFs can be in a much more concise form;
3. the notations $\begin{matrix}e\\o\end{matrix}n\lambda$ of the normalised cylindrical vector wave functions mean that the summation of both even and odd modes should be taken into account when the above integral is calculated;
4. in choosing the form of the normalised cylindrical vector functions to formulate the DGF in each region of above model, the mode matching principle at each boundary should be applied at first, and also the multiple transmissions and reflections should be taken into account.

The coefficients of $A_1^{(0)} - A_4^{(0)}, \cdots, A_1^{(p)} - A_8^{(p)}$ are unknown but can be determined by the boundary conditions at $z = z_p$ $(p = 1, 2, \cdots, N)$, i.e.,

$$\bar{e}_z \times \overline{\overline{G}}_e^{(p)}\left(\overline{R} \,|\, \overline{R}'\right) = \bar{e}_z \times \overline{\overline{G}}_e^{(p+1)}\left(\overline{R} \,|\, \overline{R}'\right) \tag{8a}$$

$$\begin{aligned} &\bar{e}_z \times \frac{1}{\mu^{(p)}}\left[\nabla \times \overline{\overline{G}}_e^{(p)}\left(\overline{R} \,|\, \overline{R}'\right) - j\omega\eta^{(p)}\overline{\overline{G}}_e^{(p)}\left(\overline{R} \,|\, \overline{R}'\right)\right] \\ &= \bar{e}_z \times \frac{1}{\mu^{(p+1)}}\left[\nabla \times \overline{\overline{G}}_e^{(p+1)}\left(\overline{R} \,|\, \overline{R}'\right) - j\omega\eta^{(p+1)}\overline{\overline{G}}_e^{(p+1)}\left(\overline{R} \,|\, \overline{R}'\right)\right], \end{aligned} \tag{8b}$$

and especially, at $z = 0$, we have

$$\bar{e}_z \times \overline{\overline{G}}_e^{(1)}\left(\overline{R} \,|\, \overline{R}'\right) = 0. \tag{9}$$

Then, by substituting (4)–(6) into (8a, b), and after tedious mathematical manipulations, two independent sets of linear equations can be derived for determining all the unknown coefficients, which are presented in Appendix 1.

On the other hand, when the grounded plane is removed in Fig. 1, and the region of $z < 0$ is assumed to be free space, the corresponding DGF should be:

$$\begin{aligned} \overline{\overline{G}}_e^{(z<0)}\left(\overline{R} \,|\, \overline{R}'\right) = \sum_{n=0}^{+\infty} \int_0^{+\infty} g^{(0)} C^{(0)} d\lambda \Big\{ \Big[& A_1^{(0-)} \overline{V}_{e_{o}^{n\lambda}}(-h_0) \\ & + A_2^{(0-)} \overline{W}_{e_{o}^{n\lambda}}(-h_0) \Big] \overline{V}'_{e_{o}^{n\lambda}}(h_0) + \Big[A_3^{(0-)} \overline{V}_{e_{o}^{n\lambda}}(-h_0) \\ & + A_4^{(0-)} \overline{W}_{e_{o}^{n\lambda}}(-h_0) \Big] \overline{W}'_{e_{o}^{n\lambda}}(h_0) \Big\} \end{aligned} \tag{10}$$

where $A_1^{(0-)} - A_4^{(0-)}$ are also the unknown coefficients to be determined.

Furthermore, by substituting (2) together with (4)–(6) into (3), respectively, the electromagnetic fields excited by the thin circular loop antenna in each layer can be found as follows:

$$\overline{E}^{(0)}\left(\overline{R}\right) = \overline{E}_0^{(0)}\left(\overline{R}\right) + \overline{E}_s^{(0)}\left(\overline{R}\right) \tag{11a}$$

where

$$\overline{E}_0^{(0)}(\overline{R}) = \frac{j\omega\mu_0}{\sqrt{2}\pi}\sum_{n=0}^{+\infty}\int_0^{+\infty} g^{(0)}C^{(0)}d\lambda \cdot \begin{cases} \left[\overline{V}_{\substack{e\\o}n\lambda}(h_0)J_{V-}^{(\pm)} + \overline{W}_{\substack{e\\o}n\lambda}(h_0)J_{W-}^{(\mp)}\right], & z \geq d_0, \\ \left[\overline{V}_{\substack{e\\o}n\lambda}(-h_0)J_{V+}^{(\mp)} + \overline{W}_{\substack{e\\o}n\lambda}(-h_0)J_{W+}^{(\pm)}\right], & z_N \leq z \leq d_0; \end{cases} \tag{11b}$$

and

$$\begin{aligned}\overline{E}_s^{(0)}(\overline{R}) = \frac{j\omega\mu_0}{\sqrt{2}\pi}\sum_{n=0}^{+\infty}\int_0^{+\infty} g^{(0)}C^{(0)}d\lambda \\ \cdot\left\{\left[A_1^{(0)}\overline{V}_{\substack{e\\o}n\lambda}(h_0) + A_2^{(0)}\overline{W}_{\substack{e\\o}n\lambda}(h_0)\right]J_{V+}^{(\mp)}\right. \\ \left. + \left[A_3^{(0)}\overline{V}_{\substack{e\\o}n\lambda}(h_0) + A_4^{(0)}\overline{W}_{\substack{e\\o}n\lambda}(h_0)\right]J_{W+}^{(\pm)}\right\}\end{aligned} \tag{11c}$$

In the pth layer $(z_{p-1} \leq z \leq z_p,\ p = 1, 2, \cdots, N)$,

$$\begin{aligned}\overline{E}^{(p)}(\overline{R}) = \frac{j\omega\mu_0}{\sqrt{2}\pi}\sum_{n=0}^{+\infty}\int_0^{+\infty} g^{(0)}C^{(0)}d\lambda \\ \cdot\left\{\left[A_1^{(p)}\overline{V}_{\substack{e\\o}n\lambda}\left(-h_+^{(p)}\right) + A_2^{(p)}\overline{W}_{\substack{e\\o}n\lambda}\left(-h_-^{(p)}\right)\right]J_{V+}^{(\mp)}\right. \\ + \left[A_3^{(p)}\overline{V}_{\substack{e\\o}n\lambda}\left(-h_+^{(p)}\right) + A_4^{(p)}\overline{W}_{\substack{e\\o}n\lambda}\left(-h_-^{(p)}\right)\right]J_{W+}^{(\pm)} \\ + \left[A_5^{(p)}\overline{V}_{\substack{e\\o}n\lambda}\left(h_+^{(p)}\right) + A_6^{(p)}\overline{W}_{\substack{e\\o}n\lambda}\left(h_-^{(p)}\right)\right]J_{V+}^{(\mp)} \\ \left. + \left[A_7^{(p)}\overline{V}_{\substack{e\\o}n\lambda}\left(h_+^{(p)}\right) + A_8^{(p)}\overline{W}_{\substack{e\\o}n\lambda}\left(h_-^{(p)}\right)\right]J_{W+}^{(\pm)}\right\}\end{aligned} \tag{12}$$

and the shorthand notations in (11)–(12) are

$$J_{V+}^{(\mp)} = e^{jh_0d_0}\left[\mp\frac{jh_0n}{k_0a_1}J_n(\lambda a_1)I_{(c)}^{(s)} - \frac{dJ_n(\lambda a_1)}{da_1}I_{(s)}^{(c)}\right] \tag{13a}$$

$$J_{V-}^{(\pm)} = e^{-jh_0d_0}\left[\pm\frac{jh_0n}{k_0a_1}J_n(\lambda a_1)I_{(c)}^{(s)} - \frac{dJ_n(\lambda a_1)}{da_1}I_{(s)}^{(c)}\right] \tag{13b}$$

$$J_{W+}^{(\pm)} = e^{jh_0d_0}\left[\pm\frac{jh_0n}{k_0a_1}J_n(\lambda a_1)I_{(c)}^{(s)} - \frac{dJ_n(\lambda a_1)}{da_1}I_{(s)}^{(c)}\right] \tag{13c}$$

$$J_{W-}^{(\mp)} = e^{-jh_0 d_0}\left[\mp\frac{jh_0 n}{k_0 a_1} J_n(\lambda a_1) I_{C}^{(S)} - \frac{dJ_n(\lambda a_1)}{da_1} I_{S}^{(C)}\right] \tag{13d}$$

$$I_{S}^{(C)} = \int_0^{2\pi} \begin{matrix}\cos\\ \sin\end{matrix}(n\varphi') I(\varphi') d\varphi',\ I_{C}^{(S)} = \int_0^{2\pi} \begin{matrix}\sin\\ \cos\end{matrix}(n\varphi') I(\varphi') d\varphi' \tag{13e, f}$$

where $J_n(\lambda a_1)$ is the nth-order cylindrical Bessel function.

Correspondingly, the magnetic fields excited by the loop antenna are expressed as:

$$\overline{H}^{(0)}(\overline{R}) = \overline{H}_0^{(0)}(\overline{R}) + \overline{H}_s^{(0)}(\overline{R}) \tag{14a}$$

where

$$\begin{aligned}\overline{H}_0^{(0)}(\overline{R}) = &\frac{k_0}{\sqrt{2}\pi}\sum_{n=0}^{+\infty}\int_0^{+\infty} g^{(0)} C^{(0)} d\lambda \\ &\cdot\begin{cases}\left[\overline{V}_{\substack{e\\o}n\lambda}(h_0) J_{V-}^{(\pm)} - \overline{W}_{\substack{e\\o}n\lambda}(h_0) J_{W-}^{(\mp)}\right], & z \geq d_0 \\ \left[\overline{V}_{\substack{e\\o}n\lambda}(-h_0) J_{V+}^{(\mp)} - \overline{W}_{\substack{e\\o}n\lambda}(-h_0) J_{W+}^{(\pm)}\right], & z_N \leq z \leq d_0\end{cases}\end{aligned} \tag{14b}$$

and

$$\begin{aligned}\overline{H}_s^{(0)}(\overline{R}) = &\frac{k_0}{\sqrt{2}\pi}\sum_{n=0}^{+\infty}\int_0^{+\infty} g^{(0)} C^{(0)} d\lambda \\ &\cdot\left\{\left[A_1^{(0)}\overline{V}_{\substack{e\\o}n\lambda}(h_0) - A_2^{(0)}\overline{W}_{\substack{e\\o}n\lambda}(h_0)\right] J_{V+}^{(\mp)}\right. \\ &\left.+\left[A_3^{(0)}\overline{V}_{\substack{e\\o}n\lambda}(h_0) - A_4^{(0)}\overline{W}_{\substack{e\\o}n\lambda}(h_0)\right] J_{W+}^{(\pm)}\right\}.\end{aligned} \tag{14c}$$

In the pth layer $(z_{p-1} \leq z \leq z_p,\ p = 1, 2, \cdots, N)$,

$$\begin{aligned}\overline{H}^{(p)}(\overline{R}) = &\frac{\omega\mu_0}{\sqrt{2}\pi}\sum_{n=0}^{+\infty}\int_0^{+\infty} g^{(0)} C^{(0)} d\lambda \\ &\cdot\left\{\left[\frac{A_1^{(p)}}{Z_+^{(p)}}\overline{V}_{\substack{e\\o}n\lambda}\left(-h_+^{(p)}\right) - \frac{A_2^{(p)}}{Z_-^{(p)}}\overline{W}_{\substack{e\\o}n\lambda}\left(-h_-^{(p)}\right)\right] J_{V+}^{(\mp)}\right. \\ &\left.+\left[\frac{A_3^{(p)}}{Z_+^{(p)}}\overline{V}_{\substack{e\\o}n\lambda}\left(-h_+^{(p)}\right) - \frac{A_4^{(p)}}{Z_-^{(p)}}\overline{W}_{\substack{e\\o}n\lambda}\left(-h_-^{(p)}\right)\right] J_{W+}^{(\pm)}\right.\end{aligned}$$

$$+\left[\frac{A_5^{(p)}}{Z_+^{(p)}}\overline{V}_{\delta}^{e}{}_{n\lambda}\left(h_+^{(p)}\right)-\frac{A_6^{(p)}}{Z_-^{(p)}}\overline{W}_{\delta}^{e}{}_{n\lambda}\left(h_-^{(p)}\right)\right]J_{V+}^{(\mp)}$$
$$+\left[\frac{A_7^{(p)}}{Z_+^{(p)}}\overline{V}_{\delta}^{e}{}_{n\lambda}\left(h_+^{(p)}\right)-\frac{A_8^{(p)}}{Z_-^{(p)}}\overline{W}_{\delta}^{e}{}_{n\lambda}\left(h_-^{(p)}\right)\right]J_{W+}^{(\pm)}\Bigg\} \quad (15)$$

and

$$Z_{\pm}^{(p)}=\frac{1}{\varepsilon^{(p)}}\left\{\pm\frac{j\left[\xi^{(p)}+\eta^{(p)}\right]}{2}+\sqrt{\varepsilon^{(p)}\mu^{(p)}-\frac{\left[\xi^{(p)}+\eta^{(p)}\right]^2}{4}}\right\} \quad (16a,b)$$

are the characteristic impedances of RCP (+) and LCP (−) modes in the pth chiral layer, respectively. In fact, $Z_{\pm}^{(p)}=\sqrt{\dfrac{\mu^{(p)}}{\varepsilon^{(p)}}}$ under the condition of $\xi^{(p)}=\eta^{(p)*}=j\kappa^{(p)}$. Here the field expressions (11), (12), (14) and (15) are valid for any current distributions on the circular loop antenna and any observation point except for the regions occupied by the loop itself. Naturally, the scalar forms of all field components with respect to the cylindrical coordinate system $(r,\ \varphi,\ z)$ can also be derived but are suppressed here. Now we pay attention to the following current distributions:

1. Fourier series distribution [30, 32], i.e.,

$$I(\varphi')=I_0+\sum_{s=1}^{\infty}I_s\cos(s\varphi') \quad (17)$$

For such a non-uniform distribution, substituting (17) into (13c, d), the above shorthand notations (13a, b) are reduced to be

$$J_{V+}^{(\mp)}=\pi(1+\delta_{n0})I_n e^{jh_0d_0}\left[\mp\frac{jh_0n}{k_0a_1}J_n(\lambda a_1)\begin{pmatrix}0\\1\end{pmatrix}-\frac{dJ_n(\lambda a_1)}{da_1}\begin{pmatrix}1\\0\end{pmatrix}\right] \quad (18a)$$
$$J_{V-}^{(\pm)}=\pi(1+\delta_{n0})I_n e^{-jh_0d_0}\left[\pm\frac{jh_0n}{k_0a_1}J_n(\lambda a_1)\begin{pmatrix}0\\1\end{pmatrix}-\frac{dJ_n(\lambda a_1)}{da_1}\begin{pmatrix}1\\0\end{pmatrix}\right] \quad (18b)$$
$$J_{W+}^{(\pm)}=\pi(1+\delta_{n0})I_n e^{jh_0d_0}\left[\pm\frac{jh_0n}{k_0a_1}J_n(\lambda a_1)\begin{pmatrix}0\\1\end{pmatrix}-\frac{dJ_n(\lambda a_1)}{da_1}\begin{pmatrix}1\\0\end{pmatrix}\right] \quad (18c)$$
$$J_{W-}^{(\mp)}=\pi(1+\delta_{n0})I_n e^{-jh_0d_0}\left[\mp\frac{jh_0n}{k_0a_1}J_n(\lambda a_1)\begin{pmatrix}0\\1\end{pmatrix}-\frac{dJ_n(\lambda a_1)}{da_1}\begin{pmatrix}1\\0\end{pmatrix}\right] \quad (18d)$$

Furthermore, by substituting (18a–d) into (11), (12), (14) and (15), all field expressions can be changed into another form. For example, when $z \geq d_0$,

$$\begin{aligned}
\overline{E}^{(0)}(\overline{R}) = & -\frac{j\omega\mu_0}{\sqrt{2}} \sum_{n=0}^{+\infty} I_n(1+\delta_{n0}) \int_0^{+\infty} g^{(0)} C^{(0)} d\lambda \\
& \cdot \Big\{ e^{-jh_0 d_0} dJ^{(a_1)} \left[\overline{V}_{en\lambda}(h_0) + \overline{W}_{en\lambda}(h_0) \right] \\
& + e^{-jh_0 d_0} \frac{jh_0 n}{k_0 a_1} J^{(a_1)} \left[\overline{V}_{on\lambda}(h_0) - \overline{W}_{on\lambda}(h_0) \right] \\
& + e^{jh_0 d_0} dJ^{(a_1)} \Big[\left(A_1^{(0)} + A_3^{(0)} \right) \overline{V}_{en\lambda}(h_0) \\
& + \left(A_2^{(0)} + A_4^{(0)} \right) \overline{W}_{en\lambda}(h_0) \Big] \\
& - e^{jh_0 d_0} \frac{jh_0 n}{k_0 a_1} J^{(a_1)} \Big[\left(A_1^{(0)} - A_3^{(0)} \right) \overline{V}_{on\lambda}(h_0) \\
& + \left(A_2^{(0)} - A_4^{(0)} \right) \overline{W}_{on\lambda}(h_0) \Big] \Big\} \qquad (19a)
\end{aligned}$$

$$\begin{aligned}
\overline{H}^{(0)}(\overline{R}) = & -\frac{k_0}{\sqrt{2}} \sum_{n=0}^{+\infty} I_n(1+\delta_{n0}) \int_0^{+\infty} g^{(0)} C^{(0)} d\lambda \\
& \cdot \Big\{ e^{-jh_0 d_0} dJ^{(a_1)} \left[\overline{V}_{en\lambda}(h_0) - \overline{W}_{en\lambda}(h_0) \right] \\
& + e^{-jh_0 d_0} \frac{jh_0 n}{k_0 a_1} J^{(a_1)} \left[\overline{V}_{on\lambda}(h_0) + \overline{W}_{on\lambda}(h_0) \right] \\
& + e^{jh_0 d_0} dJ^{(a_1)} \Big[\left(A_1^{(0)} + A_3^{(0)} \right) \overline{V}_{en\lambda}(h_0) \\
& - \left(A_2^{(0)} + A_4^{(0)} \right) \overline{W}_{en\lambda}(h_0) \Big] \\
& - e^{jh_0 d_0} \frac{jh_0 n}{k_0 a_1} J^{(a_1)} \Big[\left(A_1^{(0)} - A_3^{(0)} \right) \overline{V}_{on\lambda}(h_0) \\
& - \left(A_2^{(0)} - A_4^{(0)} \right) \overline{W}_{on\lambda}(h_0) \Big] \Big\} \qquad (19b)
\end{aligned}$$

$$\begin{aligned}
E^{(p)}(\overline{R}) = & -\frac{j\omega\mu_0}{\sqrt{2}} \sum_{n=0}^{+\infty} I_n(1+\delta_{n0}) \int_0^{+\infty} g^{(0)} C^{(0)} d\lambda \\
& \cdot \Big\{ e^{jh_0 d_0} dJ^{(a_1)} \Big[\left(A_1^{(p)} + A_3^{(p)} \right) \overline{V}_{en\lambda} \left(-h_+^{(p)} \right) \\
& + \left(A_2^{(p)} + A_4^{(p)} \right) \overline{W}_{en\lambda} \left(-h_-^{(p)} \right) + \left(A_5^{(p)} + A_7^{(p)} \right) \overline{V}_{en\lambda} \left(h_+^{(p)} \right)
\end{aligned}$$

$$+\left(A_6^{(p)}+A_8^{(p)}\right)\overline{W}_{en\lambda}\left(h_-^{(p)}\right)\Big]$$
$$-e^{jh_0d_0}\frac{jh_0n}{k_0a_1}J^{(a_1)}\Big[\left(A_1^{(p)}-A_3^{(p)}\right)\overline{V}_{on\lambda}\left(-h_+^{(p)}\right)$$
$$+\left(A_2^{(p)}-A_4^{(p)}\right)\overline{W}_{on\lambda}\left(-h_-^{(p)}\right)$$
$$+\left(A_5^{(p)}-A_7^{(p)}\right)\overline{V}_{on\lambda}\left(h_+^{(p)}\right)$$
$$+\left(A_6^{(p)}-A_8^{(p)}\right)\overline{W}_{on\lambda}\left(h_-^{(p)}\right)\Big]\Big\} \tag{20a}$$

$$\overline{H}^{(p)}\left(\overline{R}\right)=-\frac{\omega\mu_0}{\sqrt{2}}\sum_{n=0}^{+\infty}I_n(1+\delta_{n0})\int_0^{+\infty}g^{(0)}C^{(0)}d\lambda$$
$$\cdot\Bigg\{e^{jh_0d_0}dJ^{(a_1)}\Bigg[\frac{1}{Z_+^{(p)}}\left(A_1^{(p)}+A_3^{(p)}\right)\overline{V}_{en\lambda}\left(-h_+^{(p)}\right)$$
$$-\frac{1}{Z_-^{(p)}}\left(A_2^{(p)}+A_4^{(p)}\right)\overline{W}_{en\lambda}\left(-h_-^{(p)}\right)$$
$$+\frac{1}{Z_+^{(p)}}\left(A_5^{(p)}+A_7^{(p)}\right)\overline{V}_{en\lambda}\left(h_+^{(p)}\right)$$
$$-\frac{1}{Z_-^{(p)}}\left(A_6^{(p)}+A_8^{(p)}\right)\overline{W}_{en\lambda}\left(h_-^{(p)}\right)\Bigg]$$
$$-e^{jh_0d_0}\frac{jh_0n}{k_0a_1}J^{(a_1)}\Bigg[\frac{1}{Z_+^{(p)}}\left(A_1^{(p)}-A_3^{(p)}\right)\overline{V}_{on\lambda}\left(-h_+^{(p)}\right)$$
$$-\frac{1}{Z_-^{(p)}}\left(A_2^{(p)}-A_4^{(p)}\right)\overline{W}_{on\lambda}\left(-h_-^{(p)}\right)$$
$$+\frac{1}{Z_+^{(p)}}\left(A_5^{(p)}-A_7^{(p)}\right)\overline{V}_{on\lambda}\left(h_+^{(p)}\right)$$
$$-\frac{1}{Z_-^{(p)}}\left(A_6^{(p)}-A_8^{(p)}\right)\overline{W}_{on\lambda}\left(h_-^{(p)}\right)\Bigg]\Bigg\} \tag{20b}$$

where $J^{(a_1)}=J_n(\lambda a_1)$, and $dJ^{(a_1)}=\dfrac{dJ_n(\lambda a_1)}{da_1}$. In addition, when the thin circular loop antennas is excited by a sinusoidal current, i.e.,

$$I(\varphi')=I_s\cos(s\varphi') \tag{21}$$

the electromagnetic fields in both near and far field zones can be obtained only by replacing the factor I_n in (19)–(20) by $I_n=I_s\delta_{ns}$, and

$$\delta_{ns} = \begin{cases} 1 & n = s \\ 0 & n \neq s \end{cases}.$$

2. Uniform current distribution [30–32], i.e.,

$$I(\varphi') = I_0. \tag{22}$$

This can also be regarded as the special case of $s = 0$ shown in (17). For such a uniform current excitation, both the electric and the magnetic fields in each layer of the grounded multi-layered chiral slabs do not include the odd-mode component since $n = 0$. Therefore, the above field expressions (19a, b) and (20a, b) can be greatly simplified as follows:

$$\begin{aligned} \overline{E}^{(0)}(\overline{R}) = & -j\sqrt{2}\omega\mu_0 I_0 \int_0^{+\infty} g^{(0)} C^{(0)} d\lambda \\ & \cdot \Big\{ e^{-jh_0 d_0} dJ^{(a_1)} \left[\overline{V}_{e0\lambda}(h_0) + \overline{W}_{e0\lambda}(h_0) \right] \\ & + e^{jh_0 d_0} dJ^{(a_1)} \Big[\left(A_1^{(0)} + A_3^{(0)} \right) \overline{V}_{e0\lambda}(h_0) \\ & + \left(A_2^{(0)} + A_4^{(0)} \right) \overline{W}_{e0\lambda}(h_0) \Big] \Big\} \quad z \geq d_0, \end{aligned} \tag{23a}$$

$$\begin{aligned} \overline{H}^{(0)}(\overline{R}) = & -\sqrt{2} k_0 I_0 \int_0^{+\infty} g^{(0)} C^{(0)} d\lambda \\ & \cdot \Big\{ e^{-jh_0 d_0} dJ^{(a_1)} \left[\overline{V}_{e0\lambda}(h_0) - \overline{W}_{e0\lambda}(h_0) \right] \\ & + e^{jh_0 d_0} dJ^{(a_1)} \Big[\left(A_1^{(0)} + A_3^{(0)} \right) \overline{V}_{e0\lambda}(h_0) \\ & - \left(A_2^{(0)} + A_4^{(0)} \right) \overline{W}_{e0\lambda}(h_0) \Big] \Big\} \quad z \geq d_0, \end{aligned} \tag{23b}$$

and $(z_{p-1} \leq z \leq z_p,\ p = 1, 2, \cdots, N)$,

$$\begin{aligned} E^{(p)}(\overline{R}) = & -j\sqrt{2}\omega\mu_0 I_0 \int_0^{+\infty} g^{(0)} C^{(0)} d\lambda \\ & \cdot \Big\{ e^{jh_0 d_0} dJ^{(a_1)} \Big[\left(A_1^{(p)} + A_3^{(p)} \right) \overline{V}_{e0\lambda} \left(-h_+^{(p)} \right) \\ & + \left(A_2^{(p)} + A_4^{(p)} \right) \overline{W}_{e0\lambda} \left(-h_-^{(p)} \right) \end{aligned}$$

$$+\left(A_5^{(p)}+A_7^{(p)}\right)\overline{V}_{e0\lambda}\left(h_+^{(p)}\right)$$
$$+\left(A_6^{(p)}+A_8^{(p)}\right)\overline{W}_{e0\lambda}\left(h_-^{(p)}\right)\Big]\Big\}, \tag{24a}$$

$$\overline{H}^{(p)}(\overline{R}) = -\sqrt{2}\omega\mu_0 I_0 \int_0^{+\infty} g^{(0)}C^{(0)}d\lambda$$
$$\cdot\left\{e^{jh_0d_0}dJ^{(a_1)}\left[\frac{1}{Z_+^{(p)}}\left(A_1^{(p)}+A_3^{(p)}\right)\overline{V}_{e0\lambda}\left(-h_+^{(p)}\right)\right.\right.$$
$$-\frac{1}{Z_-^{(p)}}\left(A_2^{(p)}+A_4^{(p)}\right)\overline{W}_{e0\lambda}\left(-h_-^{(p)}\right)$$
$$+\frac{1}{Z_+^{(p)}}\left(A_5^{(p)}+A_7^{(p)}\right)\overline{V}_{e0\lambda}\left(h_+^{(p)}\right)$$
$$\left.\left.-\frac{1}{Z_-^{(p)}}\left(A_6^{(p)}+A_8^{(p)}\right)\overline{W}_{e0\lambda}\left(h_-^{(p)}\right)\right]\right\}. \tag{24b}$$

4. EVALUATION OF THE FAR ZONE FIELDS

Mathematically, the above integration in (23) and (24) with respect to λ in the range $[0,\ +\infty)$ can be extended to the range $(-\infty,\ +\infty)$ using the following relation:

$$\int_0^{+\infty} f(\lambda)J_n(\lambda)d\lambda = \int_0^{+\infty} f(\lambda)H_n^{(1)}(\lambda)d\lambda \tag{25}$$

where $H_n^{(1)}(\lambda)$ is the nth-order cylindrical Hankel function of the first kind. So in the region $z > d_0$,

$$\overline{E}^{(0)}(\overline{R}) = -\frac{j\omega\mu_0}{\sqrt{2}}\sum_{n=0}^{+\infty} I_n(1+\delta_{n0})\int_0^{+\infty} g^{(0)}C^{(0)}d\lambda$$
$$\cdot\Big\{e^{-jh_0d_0}dH^{(a_1)}\left[\overline{V}_{en\lambda}^{(1)}(h_0)+\overline{W}_{en\lambda}^{(1)}(h_0)\right]$$
$$+e^{-jh_0d_0}\frac{jh_0n}{k_0a_1}H^{(a_1)}\left[\overline{V}_{on\lambda}^{(1)}(h_0)-\overline{W}_{on\lambda}^{(1)}(h_0)\right]$$
$$+e^{jh_0d_0}dH^{(a_1)}\left[\left(A_1^{(0)}+A_3^{(0)}\right)\overline{V}_{en\lambda}^{(1)}(h_0)\right.$$

$$+\left(A_2^{(0)}+A_4^{(0)}\right)\overline{W}_{en\lambda}^{(1)}(h_0)\Big]$$
$$-e^{jh_0d_0}\frac{jh_0n}{k_0a_1}H^{(a_1)}\left[\left(A_1^{(0)}-A_3^{(0)}\right)\overline{V}_{on\lambda}^{(1)}(h_0)\right.$$
$$\left.+\left(A_2^{(0)}-A_4^{(0)}\right)\overline{W}_{on\lambda}^{(1)}(h_0)\right]\Big\}, \tag{26a}$$

$$\overline{H}^{(0)}(\overline{R}) = -\frac{k_0}{\sqrt{2}}\sum_{n=0}^{+\infty}I_n(1+\delta_{n0})\int_0^{+\infty}g^{(0)}C^{(0)}d\lambda$$
$$\cdot\Big\{e^{-jh_0d_0}dH^{(a_1)}\left[\overline{V}_{en\lambda}^{(1)}(h_0)-\overline{W}_{en\lambda}^{(1)}(h_0)\right]$$
$$+e^{-jh_0d_0}\frac{jh_0n}{k_0a_1}H^{(a_1)}\left[\overline{V}_{on\lambda}^{(1)}(h_0)+\overline{W}_{on\lambda}^{(1)}(h_0)\right]$$
$$+e^{jh_0d_0}dH^{(a_1)}\left[\left(A_1^{(0)}+A_3^{(0)}\right)\overline{V}_{en\lambda}^{(1)}(h_0)\right.$$
$$\left.-\left(A_2^{(0)}+A_4^{(0)}\right)\overline{W}_{en\lambda}^{(1)}(h_0)\right]$$
$$-e^{jh_0d_0}\frac{jh_0n}{k_0a_1}H^{(a_1)}\left[\left(A_1^{(0)}-A_3^{(0)}\right)\overline{V}_{on\lambda}^{(1)}(h_0)\right.$$
$$\left.-\left(A_2^{(0)}-A_4^{(0)}\right)\overline{W}_{on\lambda}^{(1)}(h_0)\right]\Big\}, \tag{26b}$$

where $H^{(a_1)}=H_n^{(1)}(\lambda a_1)$, and $dH^{(a_1)}=\dfrac{dH_n^{(1)}(\lambda a_1)}{da_1}$. Especially, in the far field zone $(\lambda r\gg 1)$,

$$\overline{V}_{\substack{e\\o}n\lambda}^{(1)}(h_0)\approx\sqrt{\frac{\lambda}{\pi r}}e^{j\left[\lambda r+h_0z-j\frac{(2n+1)\pi}{4}\right]}\begin{matrix}\cos\\ \sin\end{matrix}(n\varphi)$$
$$\cdot\left(-j\bar{e}_\varphi+\frac{\lambda\bar{e}_z-h_0\bar{e}_r}{k_0}\right), \tag{27}$$

$$\overline{W}_{\substack{e\\o}n\lambda}^{(1)}(h_0)\approx\sqrt{\frac{\lambda}{\pi r}}e^{j\left[\lambda r+h_0z-j\frac{(2n+1)\pi}{4}\right]}\begin{matrix}\cos\\ \sin\end{matrix}(n\varphi)$$
$$\cdot\left(-j\bar{e}_\varphi-\frac{\lambda\bar{e}_z-h_0\bar{e}_r}{k_0}\right). \tag{28}$$

Furthermore, by substituting (27) and (28) into (26a,b), the integration is evaluated by means of the technique of saddle-point integration, i.e.,

$$\int_\Omega g(h)e^{jkf(h)}dh=\left[\frac{\pi}{2kf''(h_0)}\right]^{\frac{1}{2}}g(h_0)e^{j\left[kf(h_0)-\frac{\pi}{4}\right]} \tag{29}$$

where Ω stands for the steepest-decent path. It is then found that,

$$\begin{aligned}
\overline{E}^{(0)}(\overline{R}) \approx & -\frac{\omega\mu_0 k_0}{2R} e^{jk_0 R}\cos\theta \sum_{n=0}^{+\infty} I_n\,(1+\delta_{n0})\, g^{(0)} C^{(0)} e^{-j\frac{(n+1)\pi}{2}} \\
& \cdot \Big\{ j2e^{-jh_0 d_0} dH^{(a_1)}\cos(n\varphi)\bar{e}_\varphi + 2e^{-jh_0 d_0}\frac{jh_0 n}{k_0 a_1} H^{(a_1)}\sin(n\varphi)\bar{e}_\theta \\
& + e^{jh_0 d_0} dH^{(a_1)}\cos(n\varphi)\Big[\Big(A_1^{(0)}+A_3^{(0)}\Big)\overline{C}_+ - \Big(A_2^{(0)}+A_4^{(0)}\Big)\overline{C}_-\Big] \\
& - e^{jh_0 d_0}\frac{jh_0 n}{k_0 a_1} H^{(a_1)}\sin(n\varphi) \\
& \cdot \Big[\Big(A_1^{(0)} - A_3^{(0)}\Big)\overline{C}_+ - \Big(A_2{}^{(0)} - A_4^{(0)}\Big)\overline{C}_-\Big]\Big\}, \qquad (30)
\end{aligned}$$

$$\begin{aligned}
\overline{H}^{(0)}(\overline{R}) \approx & \frac{jk_0^2}{2R} e^{jk_0 R}\cos\theta \sum_{n=0}^{+\infty} I_n\,(1+\delta_{n0})\, g^{(0)} C^{(0)} e^{-j\frac{(n+1)\pi}{2}} \\
& \cdot \Big\{ 2e^{-jh_0 d_0} dH^{(a_1)}\cos(n\varphi)\bar{e}_\theta + j2e^{-jh_0 d_0}\frac{jh_0 n}{k_0 a_1} H^{(a_1)}\sin(n\varphi)\bar{e}_\varphi \\
& + e^{jh_0 d_0} dH^{(a_1)}\cos(n\varphi)\Big[\Big(A_1^{(0)}+A_3^{(0)}\Big)\overline{C}_+ + \Big(A_2^{(0)}+A_4^{(0)}\Big)\overline{C}_-\Big] \\
& - e^{jh_0 d_0}\frac{jh_0 n}{k_0 a_1} H^{(a_1)}\sin(n\varphi) \\
& \cdot \Big[\Big(A_1^{(0)} - A_3^{(0)}\Big)\overline{C}_+ + \Big(A_2{}^{(0)} - A_4^{(0)}\Big)\overline{C}_-\Big]\Big\}, \qquad (31)
\end{aligned}$$

where $h_0 = k_0\cos\theta$, $\lambda = k_0\sin\theta$, and $\overline{C}_\pm = \bar{e}_\theta \pm j\bar{e}_\varphi$. Obviously, the radiated fields are just the combination of RCP and LCP modes. But, it should be pointed out that the effects of proximity that occurs when the saddle point is near the singularities of the coefficients $A_1^{(0)} - A_4^{(0)}$ have not been taken into account, and this means that the radiated fields (30) and (31) contain only the contribution of the space wave and are not valid for observation points such that θ is equal to $\pm 90^\circ$. On the other hand, it should be emphasised that no confinement has been put on the radii of thin circular loop antennas, so (30) and (31) are applicable for both electrically large and small size cases. In addition, for the uniform-current excitation, we have,

$$\begin{aligned}
\overline{E}^{(0)}(\overline{R}) \approx & \frac{\omega\mu_0 I_0}{4\pi R} e^{jk_0 R} H_1^{(1)}(\lambda a_1) \\
& \cdot \Big\{ j2e^{-jh_0 d_0}\bar{e}_\varphi + e^{jh_0 d_0}\Big[\Big(A_1^{(0)} + A_3^{(0)}\Big)\overline{C}_+
\end{aligned}$$

$$- \left(A_2^{(0)} + A_4^{(0)}\right) \overline{C}_- \Big] \Big\}, \tag{32}$$

$$\overline{H}^{(0)}(\overline{R}) \approx - \frac{jk_0 I_0}{4\pi R} e^{jk_0 R} H_1^{(1)}(\lambda a_1) \cdot \Big\{ 2e^{-jh_0 d_0} \overline{e}_\theta + e^{jh_0 d_0} \Big[\left(A_1^{(0)} + A_3^{(0)}\right) \overline{C}_+ + \left(A_2^{(0)} + A_4^{(0)}\right) \overline{C}_- \Big] \Big\}. \tag{33}$$

5. NUMERICAL RESULTS

The normalised far-field patterns of the thin circular loop antenna above some (un)grounded chiral slabs configurations will be presented in this section. Actually, the constitutive parameters of chiral materials are the function of the operating frequency, respectively, but the parameters assumed are all in a physically realizable range. When $k_0 a_1 = 6$, the current distribution of the circular loop is described by the Fourier cosine series as in [33]:

$$\begin{aligned} I(\varphi') = {} & \left(3.361 \times 10^{-5} - j1.499 \times 10^{-4}\right) \\ & + \left(7.500 \times 10^{-5} - j1.829 \times 10^{-4}\right) \cos\varphi' \\ & + \left(2.691 \times 10^{-5} - j1.867 \times 10^{-4}\right) \cos(2\varphi') \\ & + \left(3.115 \times 10^{-5} - j2.421 \times 10^{-4}\right) \cos(3\varphi') \\ & + \left(2.058 \times 10^{-5} - j3.673 \times 10^{-4}\right) \cos(4\varphi') \\ & + \left(1.316 \times 10^{-5} - j7.540 \times 10^{-4}\right) \cos(5\varphi') \\ & + \left(8.942 \times 10^{-4} - j2.029 \times 10^{-2}\right) \cos(6\varphi') \\ & + \left(1.042 \times 10^{-7} + j8.693 \times 10^{-4}\right) \cos(7\varphi') \\ & + \left(1.198 \times 10^{-9} + j4.338 \times 10^{-4}\right) \cos(8\varphi') \\ & + \left(1.900 \times 10^{-11} + j2.917 \times 10^{-4}\right) \cos(9\varphi') \\ & + \left(3.006 \times 10^{-13} + j2.210 \times 10^{-4}\right) \cos(10\varphi'). \end{aligned} \tag{34}$$

Herein up to tenth-order harmonic current excitation with respect to the azimuth angle φ' has been taken into account. In addition, the condition $2 \ln \dfrac{2\pi a_1}{r'} = 10$ is imposed on the loop wire, where r' is the radius of wire.

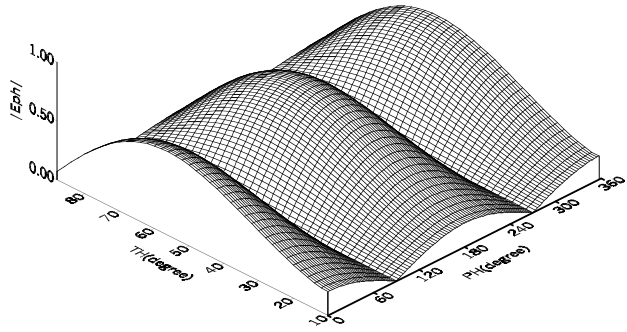

(a) First-order harmonic current excitation with respect to φ'.

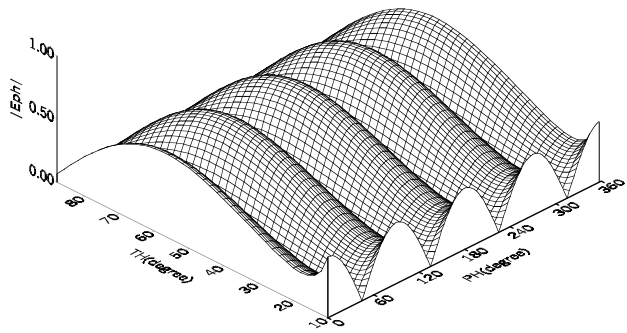

(b) Second-order harmonic current excitation with respect to φ'.

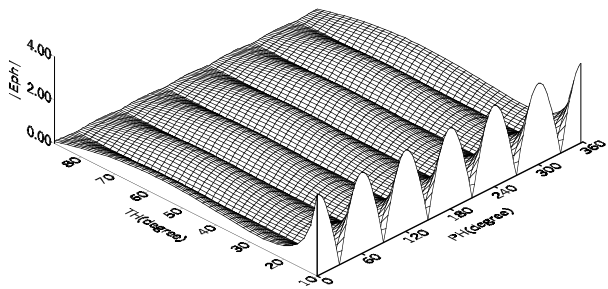

(c) Third-order harmonic current excitation with respect to φ'.

Figure 2. Three-dimensional far-zone field patterns $\left|E_{\varphi}^{(0)}\right|$ for a circular loop antenna in the presence of grounded three-layered chiral slabs.

In Figs. 2(a)–(c), the parameters chosen for calculation are $\varepsilon^{(1)} = 2.5\varepsilon_0$, $\mu^{(1)} = \mu_0$, $\kappa^{(1)} = 0.5$, $\varepsilon^{(2)} = 3.5\varepsilon_0$, $\mu^{(2)} = 1.2\mu_0$, $\kappa^{(2)} = 0.6$, $\varepsilon^{(3)} = 4.5\varepsilon_0$, $\mu^{(3)} = 1.5\mu_0$, $\kappa^{(3)} = 0.8$, $z_1/\lambda = 0.2$, $z_2/\lambda = 0.4$, $z_3/\lambda = 0.5$, $a_1/\lambda = 0.9549$, and $d_0/\lambda = 1.0$. Also (30) and (A1, 2) are employed for calculating the far-zone field components for the first-, second- and third-order harmonic current excitations, respectively. However, the losses of chiral media are neglected here. According to the image principle for chiral objects, the image effects between two circular loop antennas located up and down of six-layered chiral slabs symmetrically can also be included based on the above model, and the image parameters of the grounded three chiral slabs are characterized by $\varepsilon^{(1i)} = 2.5\varepsilon_0$, $\mu^{(1i)} = \mu_0$, $\kappa^{(1i)} = -0.5$; $\varepsilon^{(2i)} = 3.5\varepsilon_0$, $\mu^{(2i)} = 1.2\mu_0$, $\kappa^{(2i)} = -0.6$; $\varepsilon^{(3i)} = 4.5\varepsilon_0$, $\mu^{(3i)} = 1.5\mu_0$, and $\kappa^{(3i)} = -0.8$. Obviously,

(1) for the mth-order harmonic current excitation (where m can be even or odd number), there exist $2m$ resonance peaks in the azimuth angle direction and the resonance periodicity is determined by $\dfrac{\pi}{m}$;
(2) for higher order excitations, such as the fourth-, fifth- and sixth-order harmonic currents (with respect to φ'), their contributions are also important;
(3) for the uniform or the zero-order harmonic excitation, which is only applicable for the case of electrically small sized loop, all the fields are naturally have no relation to the azimuth angle φ.

As another illustrative example, Fig. 3 depicts the far-zone field pattern $\left|E_\theta^{(0)}\right|$ of the loop antenna in the presence of grounded three-layered chiral slabs. The parameters chosen for the calculation are the same as in Fig. 2(a).

In Fig. 3, only the first-order harmonic current excitation with respect to φ' is shown, and similarly, there exist 2 m peaks in the azimuth angle direction for the mth-order harmonic current excitation. When $\varphi = 90°$ and $270°$, it is noted that $\left|E_\theta^{(0)}\right|$ reaches the maximum, and when $\varphi = 0°$, $180°$ and $360°$, $\left|E_\theta^{(0)}\right| = 0.0$. On the other hand, as θ approaches $90°$, $\left|E_\theta^{(0)}\right|$ is decreased and nearly zero. Actually, chirality provides a new freedom for adjusting the relative magnitude between $E_\varphi^{(0)}$ and $E_\theta^{(0)}$, i.e., the polarized state of the far-zone or near-zone fields can be changed only by varying the chirality

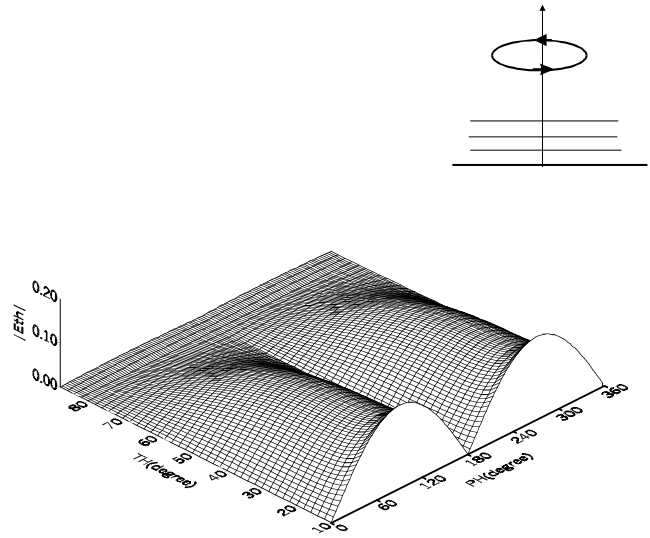

Figure 3. Three-dimensional far-zone field patterns $\left|E_{\theta}^{(0)}\right|$ for a circular loop antenna in the presence a grounded three-layered chiral slabs.

parameter, but practically, the magnitude of chirality parameter $\kappa^{(p)}$ is also governed by the other parameters of the chiral slabs. The far-zone fields $\overline{E}^{(0)}$ $\left(\overline{H}^{(0)}\right)$ are in the right- or left-handed elliptically polarized state. But in some special direction, they can be in the linear polarized state.

Fig. 4 depicts the far-zone field pattern $\left|E_{\varphi}^{(0)}\right|$ of the loop antenna in the presence of a ungrounded single layer of chiral slab for the second-order harmonic current excitation. It is known that for the ungrounded case, the far-zone fields take the same forms described by (30) and (31), except that the unknown coefficients are determined by two sets of 8×8 matrix equation for the single layer case. The parameters chosen for the calculation are $z_1/\lambda = 0.5,\ \varepsilon^{(1)} = (4.5 + i0.3)\varepsilon_0,\ \mu^{(1)} = (1.5 + i0.1)\mu_0,\ \kappa^{(1)} = 0.8,\ a_1/\lambda = 0.9549,$ and $d_0/\lambda = 0.1$; and $z < 0$ is assumed to be the free space with $(\varepsilon_0,\ \mu_0)$.

In Fig. 4, the losses of the chiral slab are taken into account, and the attenuation can not mask the variation characteristics of the far-zone fields observed as shown as in Fig. 2. With the varying of the layer number or the layer thickness, similar conclusion can be drawn for either the $E_{\varphi}^{(0)}$- or $E_{\theta}^{(0)}$-component.

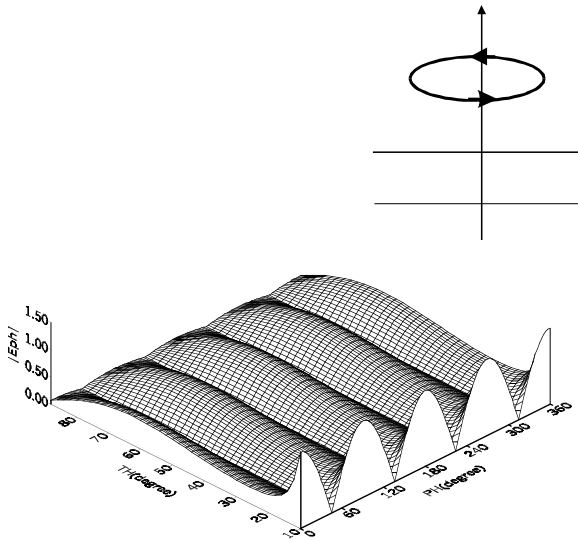

Figure 4. Three-dimensional far-zone field patterns $\left|E_{\varphi}^{(0)}\right|$ for a circular loop antenna in the presence a ungrounded single layer of chiral slab.

Finally, it should be pointed out that the current distributions employed for numerical calculations are obtained under some conditions, and the amplitudes of the lower- or higher -order harmonic currents with respect to φ' can be different if the imposed conditions are changed. However, similar resonance phenomena can be predicated even for other sets of the amplitude coefficients in (34).

6. CONCLUSIONS

The electromagnetic field excited by a thin circular loop antenna in the presence of (un)grounded chiral slabs have been characterised. The technique of dyadic Green's function expressed in terms of the normalised cylindrical vector wave functions has been imposed in the mathematical analysis. Obviously, this method is very general as well as straightforward to apply, and the loop current distribution assumed can incorporate practical applications. In particular, the formulas developed above are valid for both electrically large and small size cases in the far and near field zones, and the presented numerical results have further demonstrated the cross-polarised effects of the multi-layered chiral slabs on the radiation characteristics of sources.

APPENDIX 1

The unknown coefficients can be determined by the following equations:

$$\left[a^{(1)}\right]^T = \left[M^{(1,N)}\right]\left\{\left[M^{(0,N)}\right]\begin{bmatrix}A_1^{(0)}\\A_2^{(0)}\end{bmatrix} + \left[c_+^{(0)}\right]^T e^{-jh_0 z_n}\right\},$$

$$\left[M^{(PEC)}\right]\left[a_{1-4}^{(1)}\right]^T = [0],$$

where the superscript T stands for the transpose of a matrix,

$$\left[M^{(1,N)}\right] = \left[M^{(1,1)}\right]^{-1}\left[M^{(2,1)}\right]\cdots\left[M^{(p,p)}\right]^{-1}\left[M^{(p+1,p)}\right]\cdots\left[M^{(N,N)}\right]^{-1},$$

and

$$\left[a^{(1)}\right] = \left[A_1^{(1)}\ A_2^{(1)}\ A_5^{(1)}\ A_6^{(1)}\right], \qquad \left[c_+^{(0)}\right] = \left[1\ \frac{h_0}{k_0}\ \frac{1}{Z_0}\ \frac{h_0}{k_0 Z_0}\right]$$

$$\left[M^{(PEC)}\right] = \begin{bmatrix} 1 & 1 & 1 & 1 \\ \dfrac{h_+^{(1)}}{k_+^{(1)}} & -\dfrac{h_-^{(1)}}{k_-^{(1)}} & -\dfrac{h_+^{(1)}}{k_+^{(1)}} & \dfrac{h_-^{(1)}}{k_-^{(1)}} \end{bmatrix},$$

$$\left[M^{(0,N)}\right] = \begin{bmatrix} e^{jh_0 z_N} & e^{jh_0 z_N} \\ -\dfrac{h_0 e^{jh_0 z_N}}{k_0} & \dfrac{h_0 e^{jh_0 z_N}}{k_0} \\ \dfrac{e^{jh_0 z_N}}{Z_0} & -\dfrac{e^{jh_0 z_N}}{Z_0} \\ -\dfrac{h_0 e^{jh_0 z_N}}{k_0 Z_0} & -\dfrac{h_0 e^{jh_0 z_N}}{k_0 Z_0} \end{bmatrix},$$

$$\left[M^{(p,p)}\right] = \begin{bmatrix} e^{-jh_+^{(p)} z_p} & e^{-jh_-^{(p)} z_p} & e^{jh_+^{(p)} z_p} & e^{jh_-^{(p)} z_p} \\ \dfrac{h_+^{(p)} e^{-jh_+^{(p)} z_p}}{k_+^{(p)}} & -\dfrac{h_-^{(p)} e^{-jh_-^{(p)} z_p}}{k_-^{(p)}} & -\dfrac{h_+^{(p)} e^{jh_+^{(p)} z_p}}{k_+^{(p)}} & \dfrac{h_-^{(p)} e^{jh_-^{(p)} z_p}}{k_-^{(p)}} \\ \dfrac{e^{-jh_+^{(p)} z_p}}{Z_+^{(p)}} & -\dfrac{e^{-jh_-^{(p)} z_p}}{Z_-^{(p)}} & \dfrac{e^{jh_+^{(p)} z_p}}{Z_+^{(p)}} & -\dfrac{e^{jh_-^{(p)} z_p}}{Z_-^{(p)}} \\ \dfrac{h_+^{(p)} e^{-jh_+^{(p)} z_p}}{k_+^{(p)} Z_+^{(p)}} & \dfrac{h_-^{(p)} e^{-jh_-^{(p)} z_p}}{k_-^{(p)} Z_-^{(p)}} & -\dfrac{h_+^{(p)} e^{jh_+^{(p)} z_p}}{k_+^{(p)} Z_+^{(p)}} & -\dfrac{h_-^{(p)} e^{jh_-^{(p)} z_p}}{k_-^{(p)} Z_-^{(p)}} \end{bmatrix},$$

$$\left[M^{(p+1,p)}\right] = \begin{bmatrix} e^{-jh_+^{(p+1)}z_p} & e^{-jh_-^{(p+1)}z_p} & e^{jh_+^{(p+1)}z_p} & e^{jh_-^{(p+1)}z_p} \\ \dfrac{h_+^{(p+1)}e^{-jh_+^{(p+1)}z_p}}{k_+^{(p+1)}} & -\dfrac{h_-^{(p+1)}e^{-jh_-^{(p+1)}z_p}}{k_-^{(p+1)}} & -\dfrac{h_+^{(p+1)}e^{jh_+^{(p+1)}z_p}}{k_+^{(p+1)}} & \dfrac{h_-^{(p+1)}e^{jh_-^{(p+1)}z_p}}{k_-^{(p+1)}} \\ \dfrac{e^{-jh_+^{(p+1)}z_p}}{Z_+^{(p+1)}} & -\dfrac{e^{-jh_-^{(p+1)}z_p}}{Z_-^{(p+1)}} & \dfrac{e^{jh_+^{(p+1)}z_p}}{Z_+^{(p+1)}} & -\dfrac{e^{jh_-^{(p+1)}z_p}}{Z_-^{(p+1)}} \\ \dfrac{h_+^{(p+1)}e^{-jh_+^{(p+1)}z_p}}{k_+^{(p+1)}Z_+^{(p+1)}} & \dfrac{h_-^{(p+1)}e^{-jh_-^{(p+1)}z_p}}{k_-^{(p+1)}Z_-^{(p+1)}} & -\dfrac{h_+^{(p+1)}e^{jh_+^{(p+1)}z_p}}{k_+^{(p+1)}Z_+^{(p+1)}} & -\dfrac{h_-^{(p+1)}e^{jh_-^{(p+1)}z_p}}{k_-^{(p+1)}Z_-^{(p+1)}} \end{bmatrix},$$

$$p = 1, \cdots, N-1 \quad \text{(A1)}$$

$$\left[b^{(1)}\right]^T = \left[M^{(1,N)}\right]\left\{\left[M^{(0,N)}\right]\begin{bmatrix} A_3^{(0)} \\ A_4^{(0)} \end{bmatrix} + \left[c_-^{(0)}\right]^T e^{-jh_0 z_n}\right\},$$

$$\left[M^{(PEC)}\right]\left[b^{(1)}\right]^T = [0],$$

$$\left[b^{(1)}\right] = \left[A_3^{(1)}\ A_4^{(1)}\ A_7^{(1)}\ A_8^{(1)}\right], \quad \left[c_-^{(0)}\right] = \left[1\ -\frac{h_0}{k_0}\ -\frac{1}{Z_0}\ \frac{h_0}{k_0 Z_0}\right]. \quad \text{(A2)}$$

ACKNOWLEDGEMENT

This work was supported by the National University of Singapore under a research grant RP3981676.

REFERENCES

1. Bassiri, S., N. Engheta, and C. H. Papas, "Dyadic Green's function and dipole radiation in chiral media," *Alta Frequenza,* Vol. 55, No. 2, 83–86, 1986.
2. Engheta, N. and S. Bassiri, "One- and two-dimensional dyadic Green's function in chiral media," *IEEE Trans. Antennas Propag.,* Vol. AP-37, No. 4, 512–515, 1989.
3. Weiglhofer, W. S., "A simple and straightforward derivation of the dyadic Green's function of an isotropic chiral medium," *Arch fur Elekt. Ubertragung,* Vol. 43, No. 1, 51–52, 1989.
4. Lindell, I. V., "Simple derivation of various Green dyadics for chiral media," *Arch fur Elekt. Ubertragung,* Vol. 44, No. 5, 427–429, 1990.

5. Lakhtakia, A., "Dyadic Green's functions for an isotropic chiral half-space bounded by an anisotropic impedance plane," *Int. J. Electronics,* Vol. 72, No. 3, 493–497, 1992.
6. Lakhtakia, A., "Time-harmonic dyadic Green's functions for reflection and transmission by a chiral slab," *Arch fur Elekt. Ubertragung,* Vol. 47, No. 1, 1–5, 1993.
7. Yin, W. Y., W. B. Wang, and P. Li, "Dyadic Green's function in arbitrary multi-layered spherical chiral media and its applications," *J. Electromang. Waves Appl.,* Vol. 9, No. 1/2, 157–173, 1995.
8. Toscano, A., and L. Vegni, "Spectral dyadic Green's function formulation for planar integrated structures with a grounded chiral slab," *J. Electromang. Waves Appl.,* Vol. 6, No. 5/6, 751–770, 1992.
9. He, S., "Harmonic Green's function technique and wave propagation in stratified non-reciprocal chiral slab with multiple discontinuities," *J. Math. Phys.,* Vol. 33, No. 12, 1–8, 1992.
10. Ali, S. M., T. M. Habashy, and J. A. Kong, "Spectral-domain dyadic Green's function in layered chiral media," *J. Opt. Soc. Am. A.,* Vol. 9, No. 3, 413–423, 1992.
11. Li, L. W., P. S. Kooi, M. S. Leong, and T. S. Yao, "A general expression of dyadic Green's function in radially multi-layered chiral media," *IEEE Trans. Microwave Theory Tech.,* Vol. MTT-43, 232–238, 1995.
12. Li, L. W., P. S. Kooi, M. S. Leong, and T. S. Yao, "Analytic expression for scattering dyadic Green's function for cylindrical multilayered chiral media," *J. Electromang. Waves Appl.,* Vol. 9, 1207–1221, 1995.
13. Zhuck, N. P., O. V. Charkina, and S. N. Shul'ga, "Green's functions of Maxwell's equations for the plane-layered Tellegen biisotropic medium," *J. C.mmun. Tech. Electron.,* Vol. 41, No. 1, 22–28, 1996.
14. Hui, H.-T., and E. K. N. Yung, "The eigenfunction expansion of dyadic Green's functions for chirowaveguides," *IEEE Trans. Microwave Theory Tech.,* Vol. MTT-44, No. 9, 1575–1583, 1996.
15. Jaggard, D. L., X. Sun, and N. Engheta, "Canonical sources and duality in chiral media," *IEEE Trans. Antennas Propag.,* Vol. AP-36, No. 7, 1007–1013, 1988.
16. Jaggard, D. L., J. C. Liu, A. Grot, and P. Pelet, "Thin wire antennas in chiral media," *Electr. Lett.,* Vol. 27, No. 3, 243–244, 1991.

17. Jaggard, D. L., J. C. Liu, A. Grot, and P. Pelet, "Radiation and scattering from thin wires in chiral media," *IEEE Trans. Antennas Propag.,* Vol. AP-40, No. 11, 1273–1282, 1992.
18. Lakhtakia, A., V. V. Varadan, and V. K. Varadan, "Radiation and scattering by a straight thin-wire antenna embedded in an isotropic chiral medium," *IEEE Trans. Electromagn. Compat.,* Vol. EMC-30, No. 2, 84–87, 1988.
19. Engheta, N., and M. W. Kowarz, "Antenna radiation in the presence of a chiral sphere," *J. Appl., Phs.,* Vol. 67, No. 2, 639–646, 1990.
20. Kowarz, M. W. and N. Engheta, "Spherical chirolenses," *Opt. Lett.,* Vol. 15, No. 6, 299–302, 1992.
21. Monzon, J. C., "Radiation and scattering in homogeneous general biisotropic regions," *IEEE Trans. Antennas Propag.,* Vol. AP-38, No. 2, 227–235, 1990.
22. Yin, W. Y., and W. B. Wang, "Dyadic Green's function of cylindrical multilayered chiral media and its applications," *J. Electromang. Waves Appl.,* Vol. 7, No. 7, 1005–1027, 1993.
23. Ren, W., "Dyadic Green's functions and dipole radiations in layered chiral media," *J. Appl., Phs.,* Vol. 75, No. 1, 30–35, 1994.
24. Bhattacharyya, A. K., G. J. Burke, and E. K. Miller, "Modelling wire dipoles in an infinite chiral medium and vertically-oriented near a chiral half space," *Micro. Opt. Tech. Lett.,* Vol. 5, No. 3, 101–107, 1992.
25. Burke, G. J., E. K. Miller, and A. K. Bhattacharyya, "Current on a long, thin wire in a chiral medium," *IEEE Trans. Antennas Propag.,* Vol. AP-42, No. 6, 827–832, 1994.
26. Bhattacharyya, A. K., G. J. Burke, and E. K. Miller, "Circular loop antenna in unbounded chiral medium: a moment-method solution," *J. Electromang. Waves Appl.,* Vol. 6, No. 4, 431–444, 1992.
27. Mahmoud, S. F., "Electromagnetic fields of a current loop above a chiral half space," *J. Electromang. Waves Appl.,* Vol. 10, No. 3, 329–339, 1996.
28. Viitanen, A. J., I. V. Lindell, and A. H. Sihvola, "Polarization correction of Luneburg lens with chiral medium," *Micro. Opt. Tech. Lett.,* Vol. 3, No. 2, 62–66.
29. Viitanen, A. J., and I. V. Lindell, "Chiral slab polarization transformer for aperture antennas," *IEEE Trans. Antennas Propag.,* Vol. 46, No. 9, 1395–1397, 1998.
30. Werner, D. H., "An exact integration procedure for vector potentials of thin circular loop antennas," *IEEE Trans. Antennas Propag.,* Vol. AP-44, No. 2, 157–165, 1996.

31. Overfelt, P. L., "Near fields of the constant current thin circular loop antenna of arbitrary radius," *IEEE Trans. Antennas Propag.,* Vol. AP-44, No. 2, 166–171, 1996.
32. Li, L. W., M. S. Leong, P. S. Kooi, and T. S. Yao, "Exact solutions of electromagnetic fields in both near and far zones radiated by thin circular-loop antennas: a general representation," *IEEE Trans. Antennas Propag.,* Vol. AP-45, No. 12, 1741–1748, 1997.
33. Li, L. W., C. P. Lim, and M. S. Leong, "Method of moments analysis of electrically large circular-loop antennas: non-uniform currents," *IEE Proc-Microw. Antennas Propag.,* Vol. 147, No. 1, 2000.